

## OPTIMALLY CONVERGENT HIGH-ORDER X-FEM FOR PROBLEMS WITH VOIDS AND INCLUSIONS

Esther Sala-Lardies<sup>1</sup>, Sonia Fernández-Méndez<sup>1</sup>, and Antonio Huerta<sup>1</sup>

<sup>1</sup> Laboratori de Càlcul Numèric (LaCàN)  
Departament de Matemàtica Aplicada III, E.T.S. de Ingenieros de Caminos  
Universitat Politècnica de Catalunya, BarcelonaTECH, SPAIN  
e-mail: {esther.sala-lardies, sonia.fernandez, antonio.huerta}@upc.edu

**Keywords:** X-FEM, high-order, material interface, numerical integration

**Abstract.** *Solution of multiphase problems shows discontinuities across the material interfaces, which are usually weak. Using the eXtended Finite Element Method (X-FEM), these problems can be solved even for meshes that do not match the geometry. The basic idea is to enrich the interpolation space by means of a ridge function that is able to reproduce the discontinuity inside the elements. This approach yields excellent results for linear elements, but fails to be optimal if high-order interpolations are used.*

*In this work, we propose a formulation that ensures optimal convergence rates for bimaterial problems. The key idea is to enrich the interpolation using a Heaviside function that allows the solution to represent polynomials on both sides of the interface and, provided the interface is accurately approximated, it yields optimal convergence rates. Although the interpolation is discontinuous, the desired continuity of the solution is imposed modifying the weak form.*

*Moreover, in order to ensure optimal convergence, an accurate description of the interface (which also defines an integration rule for the elements cut by the interface) is needed. Here, we comment on different options that have been successfully used to integrate high-order X-FEM elements, and describe a general algorithm based on approximating the interface by piecewise polynomials of the same degree that the interpolation functions.*

## 1 INTRODUCTION

Although the eXtended Finite Element Method (X-FEM) was initially developed for solving fracture problems, it is nowadays widely used in many other applications, such as material inclusions, phase change or contact problems (see, for instance, [1] for an overview of the method and its applications). In particular, for problems involving several materials, discontinuities of the solution across interfaces can be represented using X-FEM, by simply enriching the interpolation.

Problems involving material interfaces yield solutions with weak discontinuities, which are usually reproduced in X-FEM using a ridge function as the ones described in [2] or [3]. These enrichments provide very good results for linear elements, but fail to be optimal if high-order interpolations are used. This problem has been recently addressed in two papers [4] and [5], where two different methods to modify integration and several ridge enrichment functions are proposed and analyzed. Both obtain optimal convergence rates for problems with voids, but not for bimaterial problems involving weak discontinuities. The goal of this paper is defining an X-FEM methodology ensuring optimal convergence for any degree.

The basic ingredients of an X-FEM method for the numerical treatment of voids or material interfaces are (i) a numerical representation of interfaces, usually described by means of level sets [6, 7] and (ii) an enrichment of the Finite Elements (FE) approximation space, to represent weak or strong discontinuities along material interfaces.

A proper representation of the interface inside the elements cut by the interface is crucial. Those elements are split by the interface in two subregions, corresponding to different materials or voids, and a separate numerical quadrature has to be defined for each subregion; to integrate only over the material domain in the case of voids, or to integrate with different material properties over each subdomain in the case of a material interface. The usual practice for first order X-FEM computations [2] is considering a linear interface representation in each cut element. This strategy provides optimal convergence rates for linear approximations, but it is clearly not suitable for high-order computations. The geometrical error due to the low resolution representation of the interface leads to poor accuracy and convergence rates limited to order  $\mathcal{O}(h^{3/2})$  in  $\mathcal{H}^1$  norm, see for instance [8].

Two main strategies have been proposed in the literature to properly represent an interface for integration purposes in  $p$ -th order computations, aiming to get rid of the effect of geometrical errors: (i) a piecewise linear representation of the interface in each cut element [5, 10] or (ii) a  $p$ -th order parametrization to approximate the interface [4]. In [5], an octree-like partition of the element in integration cells is recursively defined to get a piecewise linear representation of the interface, with segments of the desired size  $\tilde{h}$ . Special care has to be paid to the level of refinement in order to get accurate results and optimal convergence rates. In fact, optimal asymptotic convergence can not be obtained with a constant ratio  $\tilde{h}/h$  and, as noted in [5], further refinement of the integration cells is necessary as the computational mesh is refined. Numerical tests confirm the optimal convergence of this robust, and easy to implement, technique. Nevertheless, it has two important drawbacks for practical purposes: (i) the overhead in computational cost, comparable to a *linear  $h$ -refinement* around the interface, and (ii) the strong dependence of the solution accuracy on the integration cell size  $\tilde{h}$ . In practice, user decision and tuning of the integration cells size  $\tilde{h}$ , or an strategy to estimate the geometrical error in each cut element, is necessary to get a good performance for a given computational mesh. Alternatively a  $p$ -th order parametrization for the representation of the interface in each element is proposed in [4], leading to accurate results and optimal convergence rates with little overhead in computational cost.

However, the strategy proposed in [4] restricts to a simple situation, assuming that the interface cuts the element boundary in only two points at different sides. Thus, this strategy may fail in complicated situations, that can usually appear with a high-order level set, such as a bubble inside one element, or an interface cutting more than two sides of an element. To overcome this limitation, a robust and efficient strategy based on a piecewise  $p$ -th order parametrization of the interface in each element – capable to handle with complicated situations, while keeping high-order convergence rates and a low overhead in computational cost — is proposed here.

Regarding the functional approximation, when the 0-level set corresponds to a material interface, the solution may present a strong discontinuity (i.e discontinuous solution) or a weak discontinuity (i.e. continuous solution with discontinuous derivative), along the interface. In this situation the approximation is enriched in all the elements cut by the interface – that is, in the so-called *reproducing elements*– in order to reproduce the desired discontinuity. For the approximation of functions with strong discontinuities, such as a crack or the pressure in a bimaterial incompressible flow problem, the Heaviside function is widely used as enrichment function [9, 10], with easy implementation and providing optimal results for any order.

On the other hand, the enrichment of the approximation for a weak discontinuity – that is continuous function with discontinuous derivative – has been typically based on a *ridge function*, for which several definitions can be found in the literature [2, 3]. The first X-FEM proposal for material inclusions [2] considers the interpolation of the distance as enrichment function. This ridge function is different from zero in the whole domain and therefore the enrichment shape functions, corresponding to nodes at elements cut by the interface, does not only affect these enriched elements but also the neighboring ones, i.e the so-called *blending elements*. Aiming to avoid blending elements, a ridge function whose support is included in the union of the reproducing elements is proposed in [3]. This ridge function and the distance ridge function yield similar interpolation spaces for linear elements, and are suitable for first order X-FEM computations providing optimal convergence rates. However, for different reasons, both approaches fail in high-order computations, leading to clearly suboptimal convergence rates, see for instance [4]. The oscillations of the modified ridge function, due to its piecewise high-order polynomial definition, leads to highly oscillating enriched shape functions, which are far from being able to reproduce piecewise polynomials of degree greater than one. On the other hand, although the X-FEM approximation with the distance ridge function is able to reproduce high-order polynomials in the elements cut by the interface, this is not the case in the blending elements, leading to global poor accuracy results. Aiming to improve high-order X-FEM computations, alternative definitions of the ridge function and the X-FEM approximation are proposed in [11, 4, 5].

A corrected X-FEM interpolation considering a complete FEM base –that is a partition of the unity– for the enrichment also in the blending elements is proposed in [11], where a plateau function is designed to keep the original enrichment in the elements cut by the interface while maintaining a compact support. It is worth noting that this approximation has a small overhead in number of degrees of freedom due to the extra enriched nodes. Although it is not theoretically justified, numerical experiments in [4] show that the corrected X-FEM approximation, in combination a  $p$ -th order interface representation for numerical integration, leads to close to optimal convergence rates up to 3rd degree. Alternative corrected X-FEM approximations with low order FE basis for enrichment, and several enrichment terms following the philosophy of a *Partition of the Unity Method* (PUM), are also considered in [4]. However, the conclusion is that the multiple enrichment does not improve the convergence rate, despite requiring a higher computational effort, and the corrected X-FEM approximation is finally recommended.

On a parallel path, a ridge function fitting a piecewise linear representation of the interface is

considered in [5] to improve high-order X-FEM computations in triangular meshes. The ridge in each cut element is a piecewise linear function whose definition is based on the same octree-like partition in cells used for numerical integration, plus a bubble whose definition depends on the number of cut edges. This ridge function introduces the desired weak discontinuity along the piecewise linear interface, but unfortunately it also introduces many other discontinuities in the interior of the element. Thus, the resulting X-FEM approximation is clearly not able to reproduce a polynomial in each one of the two subdomains. Numerical experiments in [5] exhibit clearly suboptimal convergence rates for bimaterial problems.

In conclusion, although improved ridge functions require a non-negligible overhead in computational cost and a difficult programming in some cases, none of them is able to ensure high-order optimal convergence rates.

Here, a Heaviside enrichment is considered for both strong and weak discontinuities. High-order convergence rates for any interpolation degree  $p$  are ensured thanks to the fact that the enriched approximation is able to reproduce high-order polynomials on both sides of a discontinuity. The approximation is then discontinuous along the interface, and in the case of weak discontinuities,  $C^0$  continuity is to be imposed. A weak form introducing a consistent penalty parameter, following the ideas of Nitsche's method in the context of boundary conditions [12, 13], the Interior Penalty Method in the context of DG [14, 15], or the method for unfitted meshes in [16], is stated in Section 2.

The proposed approximation and formulation leads to optimal high-order convergence rates provided that a proper numerical integration is considered. Thus, the proposed method is completed with a robust and efficient strategy for numerical integration, based on the  $p$ -th order parametrization of interfaces introduced in [11], but able to handle complicated situations, see Section 3.

Finally, some numerical results show the optimal behavior of the method.

## 2 X-FEM DISCRETIZATION

Let us consider a domain  $\Omega \in \mathbb{R}^{n_{sd}}$  split by an interface  $\Gamma$  in two disjoint subdomains, that is  $\bar{\Omega} = \bar{\Omega}_1 \cup \bar{\Omega}_2$  and  $\Gamma = \bar{\Omega}_1 \cap \bar{\Omega}_2$ . The X-FEM approximation is defined as

$$u^h(\mathbf{x}) = \sum_{i \in \mathcal{I}} N_i(\mathbf{x})u_i + \sum_{i \in \mathcal{I}^{enr}} H(\mathbf{x})N_i^{enr}(\mathbf{x})a_i. \quad (1)$$

The first term in (1) is the standard FE approximation:  $N_i$  are the standard FE shape functions of degree  $p$ ,  $\mathcal{I}$  is the set of all FE nodes in the computational mesh and  $u_i$  are the nodal coefficients. The second term corresponds to the interpolation's enrichment, characteristic of an X-FEM formulation:  $N_i^{enr}$  are FE shape functions for the enrichment contribution and  $\mathcal{I}^{enr} \subset \mathcal{I}$  is the subset of the enriched nodes (that is nodes in the reproducing elements),  $H$  is the so-called *enrichment function* and  $a_i$  are the enrichment nodal coefficients. The shape functions used for the enrichment  $N_i^{enr}$  can be different from the basic FE basis  $N_i$ , and they are only required to be a partition of the unity in the elements cut by the interface. Here, the enrichment function  $H$  is a Heaviside function, that can be for instance defined as

$$H(\mathbf{x}) = \begin{cases} 1 & \text{for } \mathbf{x} \in \Omega_1 \\ -1 & \text{for } \mathbf{x} \in \Omega_2. \end{cases} \quad (2)$$

The X-FEM approximation is then discontinuous along the interface and, in the case of a weak discontinuity,  $C^0$  continuity is imposed introducing a consistent penalty parameter in the weak form.

**Remark 1** *It is worth noting that the enriched approximation (1) can be expressed in an alternative way as two separated approximations in each region of the computational domain, just considering a duplication of the nodes in the reproducing elements. That is, two approximations*

$$u_k^h(\mathbf{x}) = \sum_{i \in \mathcal{I}_k} N_i(\mathbf{x}) u_i \quad \text{in } \Omega_k, \quad k = 1, 2$$

*can be defined based on two meshes that overlap in the reproducing elements, with sets of nodes  $\mathcal{I}_1$  and  $\mathcal{I}_2$ . For instance, assuming that the duplicated reproducing elements are used for the approximation in  $\Omega_2$ ,  $\mathcal{I}_1$  would be the set of the nodes in the union of  $\Omega_1$  and the blending elements, and  $\mathcal{I}_2$  would be  $(\mathcal{I} \setminus \mathcal{I}_1) \cup \mathcal{I}^*$ , where  $\mathcal{I}^*$  is the new set of duplicated nodes. Obviously, the computational cost in terms of number of degree of freedom is the same for both approaches, since the size of the set of duplicated nodes,  $\mathcal{I}^*$ , coincides with the number of enrichment coefficients  $a_i$  in (1). This alternative is not as natural as (1) for its introduction in an X-FEM code, but gets rid of blending elements in the numerical integration.*

To illustrate the methodology, the weak form with consistent penalty parameter is stated next for a bimaterial elliptic problem, whose solution presents a weak discontinuity. The bimaterial elliptic problem is stated as

$$\begin{aligned} \nabla \cdot (\mu \nabla u) &= -s && \text{in } \widehat{\Omega} \\ u &= u_D && \text{on } \partial\Omega \\ \llbracket u \rrbracket &= 0 && \text{on } \Gamma \\ \llbracket \mu \nabla u \rrbracket \cdot \mathbf{n} &= 0 && \text{on } \Gamma \end{aligned} \quad (3)$$

where  $\widehat{\Omega} = \Omega_1 \cup \Omega_2$  is the union of the interior of both subdomains,  $\mu$  is the viscosity (discontinuous across the interface),  $s$  is a source term,  $u_D$  are prescribed values,  $\mathbf{n}$  is the unitary outward normal vector to  $\Omega_1$  on  $\Gamma$ , and the jump  $\llbracket \cdot \rrbracket$  operator is defined along the interface, using values from both subdomains

$$\llbracket u \rrbracket = u|_{\Omega_1} - u|_{\Omega_2} \quad \text{on } \Gamma.$$

Following for instance [16], the weak form for the bimaterial problem reads: find  $u \in \mathcal{H}^1(\widehat{\Omega})$  such that  $u = u_D$  in  $\partial\Omega$  and

$$a(u, v) = l(v) \quad \forall v \in \mathcal{H}_0^1(\widehat{\Omega}) \quad (4)$$

with

$$\begin{aligned} a(u, v) &= (\mu \nabla u, \nabla v)_{\widehat{\Omega}} - \langle \{\mu \nabla u\} \cdot \mathbf{n}, \llbracket v \rrbracket \rangle_{\Gamma} \\ &\quad - \langle \llbracket u \rrbracket, \{\mu \nabla v\} \cdot \mathbf{n} \rangle_{\Gamma} + \langle \gamma \llbracket u \rrbracket, \llbracket v \rrbracket \rangle_{\Gamma} \\ l(v) &= (v, s)_{\widehat{\Omega}}, \end{aligned} \quad (5)$$

where  $(\cdot, \cdot)_{\widehat{\Omega}}$  and  $\langle \cdot, \cdot \rangle_{\Gamma}$  denote the  $\mathcal{L}_2$  scalar product in  $\widehat{\Omega}$  and  $\Gamma$ , and  $\gamma$  is a sufficiently large parameter of order  $\mathcal{O}(h^{-1})$ , to ensure coercivity of the symmetric bilinear form  $a(\cdot, \cdot)$  (see Remarks 2 and 3). The following definitions of functional spaces are used:

$$\begin{aligned} \mathcal{H}^1(\widehat{\Omega}) &:= \{v \in \mathcal{L}_2(\Omega) \mid v|_{\Omega_i} \in \mathcal{H}^1(\Omega_i) \text{ for } i = 1, 2\} \\ \mathcal{H}_0^1(\widehat{\Omega}) &= \{v \in \mathcal{H}^1(\widehat{\Omega}) \mid v = 0 \text{ on } \partial\Omega\}. \end{aligned}$$

Finally, the mean  $\{\cdot\}$  operator is defined along the interface, using values from both subdomains

$$\{u\} = \kappa_1 u|_{\Omega_1} + \kappa_2 u|_{\Omega_2} \quad \text{on } \Gamma,$$

where  $\kappa_1$  and  $\kappa_2$  are two scalars satisfying  $\kappa_1 + \kappa_2 = 1$ , the simplest choice being  $\kappa_1 = \kappa_2 = 1/2$ .

The weak imposition of the continuity of the solution  $\llbracket u \rrbracket = 0$  along the interface  $\Gamma$  can be clearly seen in the last term of the bilinear form  $a(\cdot, \cdot)$  in (5), but it is also used in the derivation of the weak form adding the third term, which also recovers the symmetry of the bilinear form. The continuity of the normal flux  $\llbracket \mu \nabla u \rrbracket \cdot \mathbf{n} = 0$  on  $\Gamma$  is also used in the derivation of the weak form canceling terms.

**Remark 2** For  $\gamma$  large enough, the IPM bilinear form  $a(\cdot, \cdot)$  defined in (5) is continuous and coercive, that is

$$a(u, v) \leq \lll u \lll \lll v \lll \quad \forall v \in \mathcal{H}_0(\widehat{\Omega}) \quad (6)$$

and

$$m \lll v \lll \leq a(v, v) \quad \forall v \in \mathcal{H}_0(\widehat{\Omega}) \quad (7)$$

for some constant  $m > 0$  independent of the mesh size  $h$ , where

$$\lll v \lll^2 = \|\nabla v\|_{\widehat{\Omega}}^2 + \|h^{1/2} \mathbf{n} \cdot \{\nabla v\}\|_{\Gamma}^2 + \|h^{-1/2} \llbracket v \rrbracket\|_{\Gamma}^2 \quad (8)$$

and  $\|\cdot\|$  denotes the standard  $\mathcal{L}^2$  norms. These properties can be proved following standard arguments, see [17, 18] for details.

**Remark 3** Parameter  $\gamma$  in (5) is a consistent penalty, in the sense that the solution of the original problem (3) is solution of the weak form (4) and therefore, in practice moderate values of the constant parameter  $\gamma$ , of order  $\mathcal{O}(h^{-1})$  for any  $p$ , provide accurate and optimally convergent results. Thus, the formulation with a consistent parameter does not suffer the ill-conditioning problems that typically arise with non-consistent penalty techniques.

The extension of the formulation for other multimaterial problems is straightforward following the same rationale, see for instance the application of Nitsche's method for linear elasticity problems in [19].

### 3 NUMERICAL INTEGRATION

Level sets are widely used to describe interfaces, such as material interfaces, voids or moving boundaries, inside a computation domain  $\Omega$  [6, 7]. An interface  $\Gamma \subset \Omega$  is represented as the iso-zero values of a level set function  $\varphi : \Omega \rightarrow \mathbb{R}$ , that is

$$\Gamma = \{\mathbf{x} \in \Omega | \varphi(\mathbf{x}) = 0\}. \quad (9)$$

As usual in X-FEM computations, here the level set function  $\varphi$  is assumed to be given by its nodal values in the computational mesh, that is

$$\varphi(\mathbf{x}) = \sum_{i \in \mathcal{I}} \varphi_i N_i(\mathbf{x}), \quad (10)$$

where, here, the nodal values of the level set function  $\varphi_i$  correspond to the signed distance of the  $i$ -th node to the interface  $\Gamma$ .

An accurate description of the interface inside each element cut by the interface is needed to define a proper numerical integration and maintain high-order convergence.

In [4], Cheng and Fries consider a  $p$ -th order polynomial parametrization for the representation of the interface in one triangular element, splitting the element in a triangle and quadrilateral integration cells. First,  $p + 1$  points on the interface are to be found, including the intersections (assumed to be two) of the interface and the element boundary. The  $p + 1$  points are used as base points for a  $p$ -th degree polynomial parametrization approximating the interface, and dividing the element in two integration cells sharing one curved side (see figure 1).

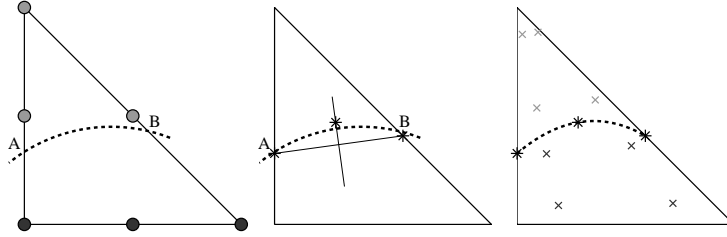


Figure 1: A quadratic triangle cut by the interface is divided in two integration cells (a triangle and a quadrilateral) sharing one curved edge.

A transformation from a straight-sided element can then be used to define the numerical quadrature in each integration cell. To avoid generating all the nodes necessary for the use of the standard isoparametric transformation, which would require a proper location of interior nodes [20], the use of specially designed transformations for elements with only one curved side is recommended here, see for instance [21]. In particular, in an element cut by an interface, parametrized by  $\phi(s)$  for  $s \in (-1, 1)$ , the following parametrizations can be used in each subdomain:

$$(\xi(s, t), \eta(s, t)) = \frac{1-t}{2}\mathbf{C} + \frac{1+t}{2}\phi(s), \quad s, t \in (-1, 1)$$

for a triangular subdomain corresponding to the convex hull of the curved side and node  $\mathbf{C}$ , and

$$(\xi(s, t), \eta(s, t)) = \frac{1-t}{2} \left[ \frac{1-s}{2}\mathbf{C} + \frac{1+s}{2}\mathbf{D} \right] + \frac{1+t}{2}\phi(s), \quad s, t \in (-1, 1)$$

for a curved quadrilateral corresponding to the convex hull of the curved size and nodes  $\mathbf{C}$  and  $\mathbf{D}$  (for a quadrilateral  $\{\phi(-1), \phi(1), \mathbf{D}, \mathbf{C}\}$  being properly oriented, or switching  $\mathbf{C}$  and  $\mathbf{D}$  otherwise).

It is worth noting that, in the case of a composite triangle quadrature, the quadrilateral curved cell can be first split, for instance, joining an intersection of the interface and the element boundary with the vertexes of the quadrilateral. A similar procedure can be defined for a quadrilateral element, that in the simpler situation, can be split by an interface in two quadrilaterals, or in one triangle and a pentagon. As in the previous case, quadrilateral or pentagonal subregions can be split in triangles or a combination of triangles and quadrilaterals, paying attention to avoid crossing of the curved side with the new sides, see Figure 2.

Numerical examples in Section 4 illustrate how the approximation of the interface with a piecewise  $p$ -th order parametrization in each element leads to optimal convergence rates, that is, errors of order  $\mathcal{O}(h^{p+1})$  in the  $\mathcal{L}_2$  norm and errors of order  $\mathcal{O}(h^p)$  in the  $\mathcal{H}^1$  seminorm.

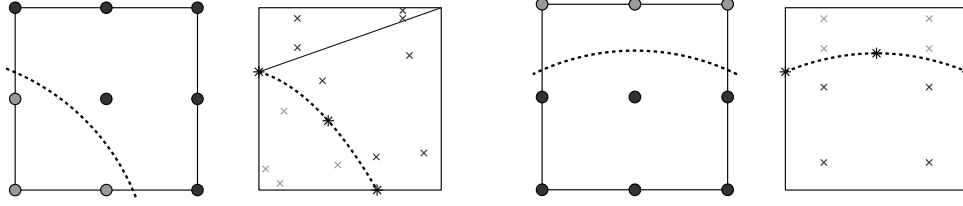


Figure 2: Two different situations for a quadrilateral split by an interface: (left) the element is divided in two triangular cells plus a quadrilateral cell, (right) the element is divided in two quadrilateral cells.

Nevertheless, the assumption of an interface cutting the element boundary in two points at different sides is too restrictive for high-order computations, and hampers the robustness of the method. High-order level sets may lead to very complex interfaces, see some examples in Figure 3, that are not contemplated in [4]. In a more general context, an interface can split an element in more than two regions. Moreover, even if it is split in only two regions, casuistic (interior bubble, two cuts in the same side, etc) may difficult the implementation of a unique  $p$ -th order polynomial parametrization.

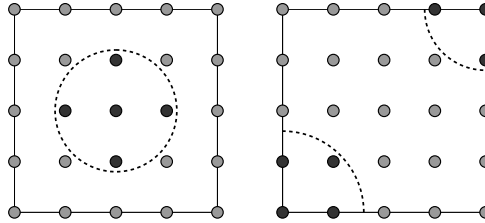


Figure 3: Some examples of interfaces described by a 4-th order level set. Nodes with different sign of the level set function are plotted with different colors.

Here a simple idea is proposed: divide and conquer. That is, any element intersected by the interface in a complex manner is recursively divided in integration cells until all cells can be considered either *basic cells* – i.e. cells whose boundary is cut by the interface twice in two different sides – or not intersected by the interface. Nodal values of the level-set function are projected from the original element to get nodal values in the integration cells. Then, the strategy considering a  $p$ -th order parametrization of the interface is applied for all *basic cells*, leading to a piecewise  $p$ -th order interface representation in the element.

**Remark 4** *The recursive division in cells must be done using the same type of element – for instance, a  $p$ -th order quadrilateral element should be split in  $p$ -th order quadrilateral cells and not triangular cells – so that the resulting level set is exactly the same polynomial level set, and no information is lost during the process.*

**Remark 5** *The recursive division in cells is done only for integration purposes –that is, to define a numerical quadrature in the original  $p$ -th order element – and it does not represent any change in the computational mesh and the corresponding number of degrees of freedom.*

For an easy implementation, the decision of splitting an element or cell can be based in the changes of sign of the level-set nodal values, first looking to nodal values at sides and then looking to interior nodal values. An element or cell is to be split if:

- (i) one of its sides is cut more than once by the interface (there are more than one changes of sign of the nodal values of the level set in the side), or



- (ii) it has more than two sides cut by the interface, or
- (iii) its boundary is not intersected by the interface, but it has one or more interior nodes with sign of the level set different to the boundary sign (interior bubble or void).

Figure 4 shows an example of recursive division and the corresponding numerical quadrature for a second order finite element. Nodal values with different sign are marked with different colors.

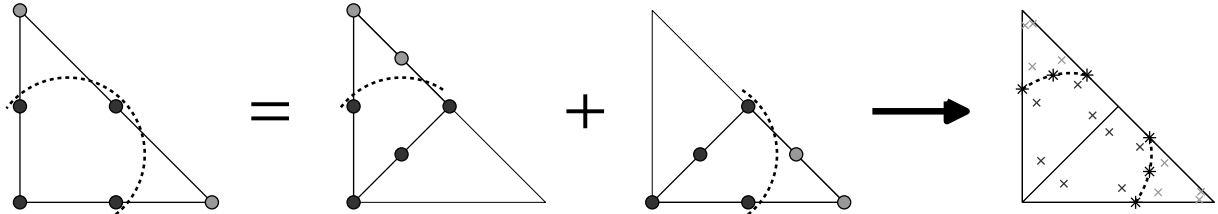


Figure 4: An element intersect by a level-set in a complex manner is divided in basic cells, which are used for integration purposes only.

The strategy considering a piecewise  $p$ -th order parametrization to approximate the interface provides optimal convergence rates for any order, in a robust manner. Moreover, in practical applications most of the elements cut by the interface will be in the *basic* situation, and paying little attention to the casuistic for the recursive division in the complex elements, they will usually be divided in few integration cells, with little overhead in computational cost.

## 4 NUMERICAL RESULTS

The behavior of the proposed methodology is analyzed in the following examples. First, a Laplace equation defined in a domain with a hole is solved to show the performance of the numerical integration strategies. Then, a bimaterial elliptic problem, with a weak discontinuity across the material interface, is solved using the Heaviside enrichment, to show that convergence is optimal for any interpolation degree.

### 4.1 Laplace equation in a domain with a hole

A Poisson problem in a domain with a hole is considered to test two different alternatives for numerical integration: the piecewise  $p$ -th order parametrization presented in Section 3, and the approach based on an octree-like partition proposed in [5]. The problem statement is

$$\begin{aligned}
 -\Delta u &= f & \text{in } \Omega &= (-1, 1)^2 \setminus B(0, 0.4) \\
 u &= g & \text{on } \partial((-1, 1)^2) \\
 \nabla u \cdot \mathbf{n} &= 0 & \text{on } \partial B(0, 0.4)
 \end{aligned} \tag{11}$$

where  $B(0, 0.4)$  is the ball of radius 0.4 centered at 0, and the source term  $f$  and prescribed values  $g$  are such that the analytical solution is  $u(x, y) = (\sqrt{x^2 + y^2} - 0.4)^2(\sin(\pi x) + 1)$ , see Figure 5.

Figure 6 shows a convergence test using the piecewise  $p$ -th order approximation of the interface, for order  $p = 1, 2, 3, 4$ . The approximation of the interface with a piecewise  $p$ -th order parametrization in each element leads to errors of order  $\mathcal{O}(h^{p+1})$  in the FE solution, ensuring the preservation of optimal convergence rates for both  $\mathcal{L}_2$  and  $\mathcal{H}^1$  norms, in a robust manner.

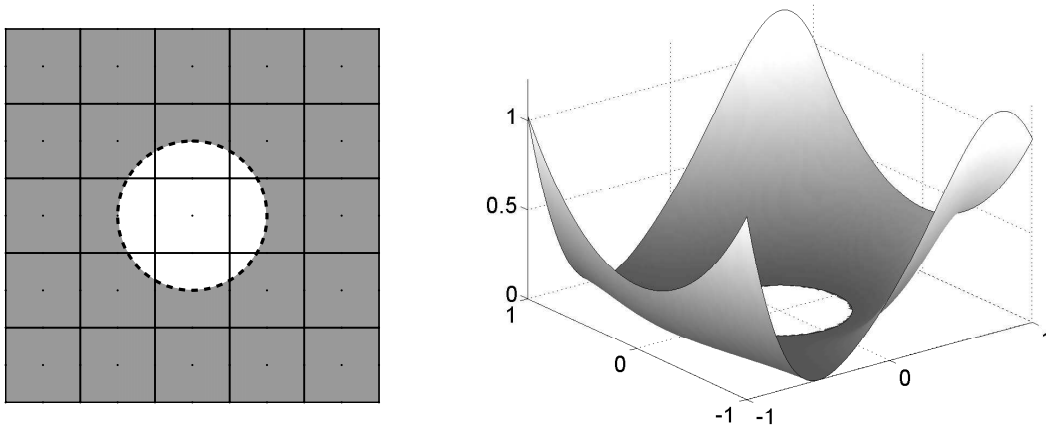


Figure 5: Example of computational mesh (left) and analytical solution for the Poisson problem in a domain with a hole (11)

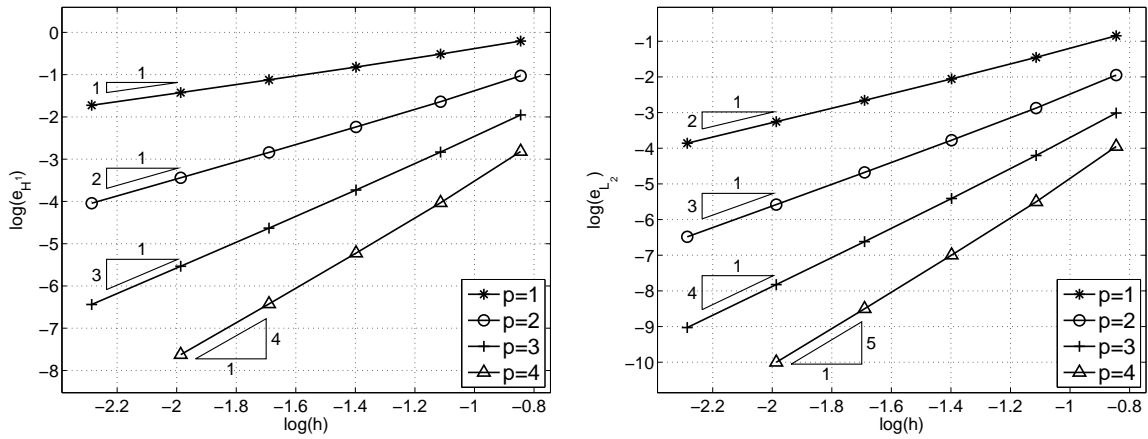


Figure 6: Convergence test with a  $p$ -th order approximation of the interface in each subelement.

Optimal convergence can also be attained with a fine enough piecewise linear approximation of the interface, based for instance in the octree-like partition in integration cells proposed in [5]. However, special care has to be paid to the level of refinement in order to get accurate results and optimal convergence rates. As noted in [5], further refinement of the integration cells is necessary as the computational mesh is refined. Figure 7 shows the evolution of the error for the solution of the Poisson problem (11) in a computational mesh with  $25 \times 25$  nodes and order  $p = 2, 3, 4$ , for decreasing integration cell size  $\tilde{h}$ . The accuracy in the solution strongly depends on the integration cell size  $\tilde{h}$ . This example illustrates that, in practice, user decision and tuning of the integration cells size  $\tilde{h}$ , or an strategy to estimate the geometrical error in each cut element, is necessary to get a good performance for a given computational mesh. Therefore, this strategy has two important drawbacks for practical purposes: (i) the overhead in computational cost, comparable to a *first order h-refinement* along the interface, and (ii) the selection of the integration cells' size for a given problem and computational mesh.

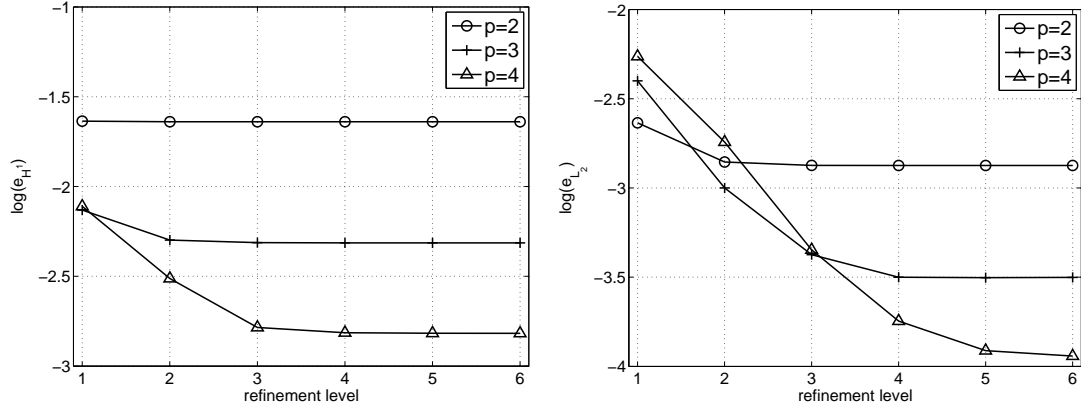


Figure 7: Evolution of the error for the solution of the Poisson problem (11) in a computational mesh with  $25 \times 25$  nodes and order  $p = 2, 3, 4$ , with increasing number of subelements for the piecewise linear representation of the interface in each element. The refinement level can be defined as the ratio between the element size  $h$  and the integration cell size  $\tilde{h}$ .

## 4.2 Bimaterial elliptic problem

The second example corresponds to the bimaterial elliptic problem (3) with  $\Omega_1 = (-1, 1)^2 \setminus B(0, 0.4)$  and  $\Omega_2 = B(0, 0.4)$ . The diffusion parameter is piecewise constant

$$\mu = \begin{cases} 1 & \text{in } \Omega_1 \\ 5 & \text{in } \Omega_2 \end{cases}$$

and the boundary conditions and source term are defined so that the exact solution is

$$u(\mathbf{x}) = \begin{cases} Ar^2 + \frac{B}{r^2} & \text{if } \mathbf{x} \in \Omega_1 \\ r^2 & \text{if } \mathbf{x} \in \Omega_2 \end{cases}$$

where  $r = \sqrt{x^2 + y^2}$ ,  $A = \frac{a(2\mu_1 + \mu_2)}{2\mu_2}$  and  $B = \frac{a^3(\mu_2 - 2\mu_1)}{2\mu_2}$  and  $a = 0.4$  is the radius of the circular inclusion (see Figure 8).

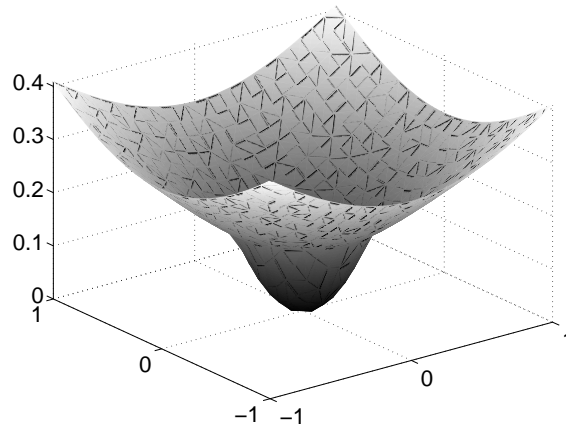


Figure 8: Exact solution for a bimaterial elliptic problem.

Figure 9 shows the convergence plots for  $\mathcal{L}_2$  norm obtained with 3-rd and 4-th order triangular elements, using different enrichment options: the ridge function proposed in [2], the modified ridge that avoids blending elements [3], the corrected X-FEM proposed in [11] and the Heaviside enrichment proposed in Section 2. It can be seen that the Heaviside enrichment provides better results than the other formulations, which are found to be sub-optimal for the 4-th degree interpolation. Numerical tests show similar results if the  $\mathcal{H}^1$  norm or quadrilateral elements are considered.

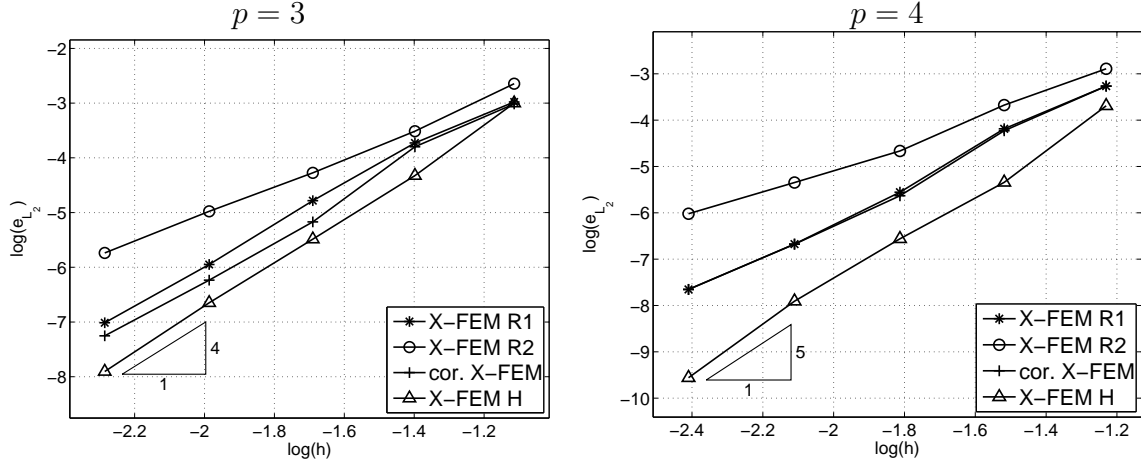


Figure 9: Convergence plot for different X-FEM enrichments, using triangular elements of degree three (left) and four (right).

Figure 10 shows the convergence plots obtained using the Heaviside formulation described in Section 2, for triangular elements up to degree  $p = 4$ . Convergence is optimal for any degree, as the same convergence rates than for standard finite elements are achieved, that is, errors of order  $\mathcal{O}(h^{p+1})$  for the  $\mathcal{L}_2$  and of order  $\mathcal{O}(h^{p+1})$  for the  $\mathcal{H}^1$  norm.

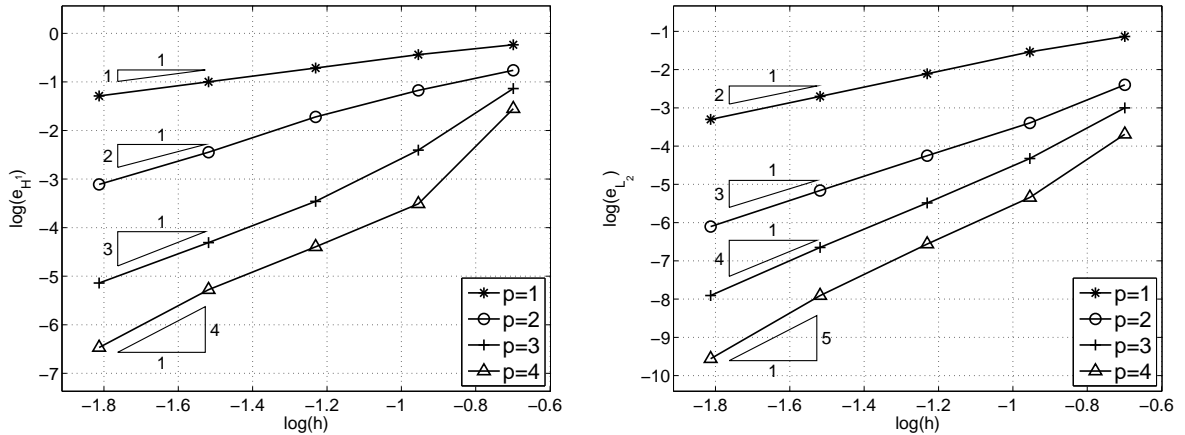


Figure 10: Convergence plots in energy and  $L_2$  norms for a bimaterial elliptic problem solved using X-FEM with a Heaviside enrichment, on a uniform mesh of triangular elements.

## 5 CONCLUDING REMARKS

An optimally convergent X-FEM formulation for solving bimaterial problems is proposed in this work. The two basic ingredients of the method are (i) an accurate representation of

the interface and (ii) a suitable enrichment function, which allows reproducing polynomials on both sides of the interface. The interface is approximated inside each element by a  $p$ -th degree polynomial parametrization. If the element is cut by the level-set in a complex manner, it can be divided until a basic situation is obtained and, in this case, the interface is approximated by a piecewise polynomial inside the element. This approximation of the interface divides the element in cells, which are used to build a composite quadrature. Regarding the interpolation, the FE space is enriched using a Heaviside function. In the case of weak discontinuities, the weak form can be modified, using a consistent penalty parameter, to impose that the solution is  $C^0$  continuous. Numerical experiments show that the proposed method provides optimally convergent solutions, for any interpolation degree, in problems involving holes and materials inclusions.

## REFERENCES

- [1] T.-P. Fries, T. Belytschko: The extended/generalized finite element method: An overview of the method and its applications. *International Journal for Numerical Methods in Engineering*, 84 (2010), 253–304.
- [2] N. Sukumar, D.L. Chopp, N. Moës, T. Belytschko: Modeling holes and inclusions by level sets in the extended finite-element method. *Computer Methods in Applied Mechanics and Engineering*, 190 (2001), 6183–6200.
- [3] N. Moës, M. Cloirec, P. Cartraud, J.-F. Remacle: A computational approach to handle complex microstructure geometries. *Computer Methods in Applied Mechanics and Engineering*, 192 (2003), 3163–3177.
- [4] K. W. Cheng, T.-P. Fries: Higher-order XFEM for curved strong and weak discontinuities. *International Journal for Numerical Methods in Engineering*, 82 (2010), 564–590.
- [5] K. Dreau, N. Chevaugeon, N. Moës: Studied X-FEM enrichment to handle material interfaces with higher order finite element. *Computer Methods for Applied Mechanics and Engineering* 199 (2010), 1922–1936.
- [6] S. Osher, R. P. Fedkiw: Level set methods: an overview and some recent results. *Journal of Computational Physics*, 169 (2001), 463–502.
- [7] J. A. Sethian: *Level Set Methods and Fast Marching Methods : Evolving Interfaces in Computational Geometry, Fluid Mechanics, Computer Vision, and Materials Science*. Cambridge University Press , 1999.
- [8] P-A Raviart, J-M Thomas: *Introduction à l’analyse numérique des équations aux dérivées partielles*, Masson, 1983.
- [9] N. Moës, J. Dolbow, T. Belytschko: A finite element method for crack growth without remeshing. *International Journal for Numerical Methods in Engineering*, 46 (1999), 131 – 150.
- [10] S. Gross, A. Reusken: An extended pressure finite element space for two-phase incompressible flows with surface tension. *Journal of Computational Physics*, 224 (2007), 40 – 58.

- [11] T.-P. Fries: A corrected XFEM approximation without problems in blending elements. *International Journal for Numerical Methods in Engineering* 75 (2008), 503–532.
- [12] J. Nitsche: Über ein Variationsprinzip zur Lösung von Dirichlet-Problemen bei Verwendung von Teilräumen die keinen Randbedingungen unterworfen sind. *Abhandlungen aus dem Mathematischen Seminar der Universität Hamburg*, 36 (1970), 9–15.
- [13] S. Fernández-Méndez, A. Huerta: Imposing essential boundary conditions in mesh-free methods. *Computer Methods in Applied Mechanics and Engineering*, 193 (2004), 1257–1275.
- [14] D. N. Arnold: An interior penalty finite element method with discontinuous elements. *SIAM Journal on Numerical Analysis*, 19 (1982), 742–760.
- [15] A. Montlaur, S. Fernández-Méndez, A. Huerta: Discontinuous Galerkin methods for the Stokes equations using divergence-free approximations. *International Journal for Numerical Methods in Fluids*, 57 (2008), 1071 – 1092.
- [16] A. Hansbo, P. Hansbo: An unfitted finite element method, based on Nitsche’s method, for elliptic interface problems. *Computer Methods for Applied Mechanics and Engineering*, 191 (2002), 5537–5552.
- [17] P. Hansbo, M. G. Larson: Discontinuous Galerkin methods for incompressible and nearly incompressible elasticity by Nitsche’s method. *Computer Methods in Applied Mechanics and Engineering*, 191 (2002), 1895–1908.
- [18] P. Hansbo, M. G. Larson: Piecewise divergence-free discontinuous Galerkin methods for stokes flow. *Communications in Numerical Methods in Engineering*, 24 (2008), 355–366.
- [19] A. Hansbo, P. Hansbo: A finite element method for the simulation of strong and weak discontinuities in solid mechanics. *Computer Methods in Applied Mechanics and Engineering*, 193 (2004), 3523–3540.
- [20] P. G. Ciarlet and P. A. Raviart: Interpolation theory over curved elements, with applications to finite element methods. *Computer Methods for Applied Mechanics and Engineering*, 1 (1972), 217–249.
- [21] R. Sevilla, S. Fernández-Méndez, A. Huerta: Comparison of high-order curved finite elements. *International Journal for Numerical Methods in Engineering*, 87 (2011), 719–734.